Proceedings of the 9th International and 49th National Conference on Fluid Mechanics and Fluid Power (FMFP)
December 14-16, 2022, IIT Roorkee, Roorkee-247667, Uttarakhand, India

FMFP2022-5443

Capillary rise in the interstices of tubes

Chitransh Atre[1], Aditya Manoj[2] and Baburaj A. Puthenveettil[1]

[1]Department of Applied Mechanics, IIT Madras, Chennai-600036, India
[2] Department of Mechanical Engineering, IIITDM Kancheepuram-600127, India

ABSTRACT

We present experimental measurements of transient capillary rise in the corners of an interstice formed between an array of tubes/rods. The capillary rise shows an initial regime where the height of the corner meniscus shows a steeper dependence of $t^{4/5}$ compared to the $t^{1/3}$ dependence in a later regime. We develop a scaling law for the later regime by minimisation of the sum of the free energy and viscous dissipation, using Onsager's principle. The obtained scaling law for the capillary height in the corner $Z_m = \left(\frac{t(\sigma\cos\theta)^2}{\rho\mu g}\right)^{1/3}$ matches the measurements in the later regime.

Keywords: Interstice, capillary rise, bulk meniscus, corner meniscus

I. INTRODUCTION

Capillary action plays an important role in many applications such as flow through porous media, textile industries, ink printing, microfluidics etc. as well as in natural process like liquid flow in soils, trees and leaves. In such flows, the main driving force for a liquid to move is provided by the surface tension. Capillary rise in a circular capillary has the bulk fluid and the meniscus rise at the same rate but in a closed geometry which include corners, the bulk fluid and the corner fluid rise at different rates. Corner rise experiments in a linear profile created by two vertical plates were done by Higuera et.al. [2]. They found that at initial stages of rise, the gravity effects are negligible and at the later stages, the viscous effects will dominate. Using lubrication approximation, they showed that the corner meniscus height to be proportional to the cube root of time. Dong et.al. [1] did experiments to study the capillary rise in a capillary with a square cross section and validated with their theory.They found that the imbibition rates are in proportion to the $(\sigma/\mu)^{1/2}$ and the velocity of imbibition is proportional to $D^{1/2}$, where D is the tube size. Previously, Ponomarenko et.al.[3] performed experiments in a quadratic corner and developed a law which mentions that the height of the corner meniscus varies as $t^{1/3}$ and to be independent of the radius of the corner, even though they did not verify this independence. Recently, Zhou and Doi [4] developed a theory for small corner rise between curved surface profiles. Their outcomes supports the results given by [3]. The most commonly occurring geometry having circular regions and corners are the interstices in between an array of tubes or rods. The dependence of corner rise in such a geometry on time and, especially on the radius of the tubes or rods is not known. In the present study, we perform experiments to measure the rise of liquid in the corners in interstices.

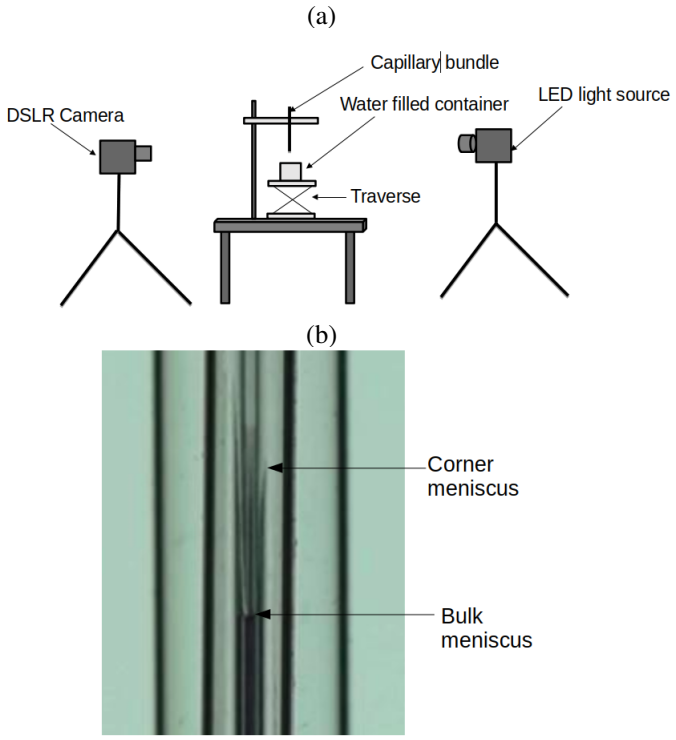

Figure 1: **(a) Schematic representation of experimental setup (b) Experimental image of water rise inside interstice of capillaries of OD = 1380 μm.**

II. EXPERIMENTAL SETUP

We use three different sizes of circular capillaries having outer diameters of 700 μm, 1380 μm and 10000 μm. Figure 1 shows a schematic diagram of the experimental setup. For each of the above diameters we used three borosilicate circular glass tubes each of 10 cm in length held together by heat shrink sleeves to create a three cornered interstice shown in the Figure 2(a). We used water mixed with blue ink to visualize the rise. The properties for water is given in the table 1. The capillary bundle was fixed vertically and a container having DI water mixed with ink was slowly brought up into contact with the bottom part of the capillary bundle with the help of traverse. As the bottom surface of the capillary touches the water surface, water rises in

the interstice. The bulk fluid as well as corner fluid rises with high rates initially with the rate of rise decreasing. When the bulk meniscus reaches equilibrium height, the corner meniscus still continues to rise due to the fact that a wetting liquid try to cover as much area of solid surface to attain minimum inter-facial energy. We record the videos of this rise using NIKON D5300 camera with 50 fps with TAMRON Macro lens of focal range 180-400mm. A LED light source was used for the back lighting. The capillary height in the corners of each capillary bundle was measured as a function of time from those videos. The Figure 1(b) shows an image frame of rise inside an interstice created by three capillaries of 1380 μm OD. The bulk meniscus and the corner meniscus tip can be seen in zoomed image.

III. METHODOLOGY

The inset in the Figure 3 shows the variations of the liquid level in the corners for each of the capillary bundle with time. There are two types of regimes that we observe. An initial regime where $h \sim t^{4/5}$ and a later regime where $h \sim t^{1/3}$. We now focus on the latter regime and find our scaling relation that collapse the data in this latter regime. In Figure 2(a), the shaded region represents the interstice which is created by joining the three circular capillaries. This interstice contains 3 sharp corners. Considering one corner, let the two surfaces that form the corner be defined by the function

$$y = \pm E(x)/2 \tag{1}$$

where,since the tube cross section is circular,

$$E(x) = 2(R - \sqrt{R^2 - x^2}) \tag{2}$$

Let the bottom of the meniscus be at $z = 0$ and the tip of the meniscus at $z = Z_m$. Figure 2(b) represents a cross sectional view of interstice. Figure 2(c) shows 3-D view with the Cartesian coordinates. Our main objective is to find the corner meniscus profile equation with respect to time.

Using Onsager's principle [4], we develop a Rayleighian function relation defined by

$$R(\dot{G}) = \dot{F}(\dot{G}) + \Phi(\dot{G}) \tag{3}$$

where $\dot{G}(z,t) = \partial G(z,t)/\partial t$, with $G(z,t)$ being the distance from the edge of corner to meniscus surface at time instant t (see Figure 2b) and $\dot{F}(\dot{G})$ represents the rate of change of free energy when the interface is moving at the rate $\dot{G}(z,t)$. Hereinafter $\cdot$ (dot) indicates derivative w.r.t. time. $\Phi(\dot{G})$ represents half of the rate of dissipation energy. $\dot{G}(z,t)$ is to be finally obtained by minimizing the function $R(\dot{G})$. Area of the interstice region, $A(G)$, in the limits $0 < x < G$ and $|y| < E(x)/2$

$$A(G) = \int_0^G E(x)dx. \tag{4}$$

Using equation (2) in (4),

$$A(G) = 2RG - G\sqrt{R^2 - G^2} + R^2 \sin^{-1} G/R. \tag{5}$$

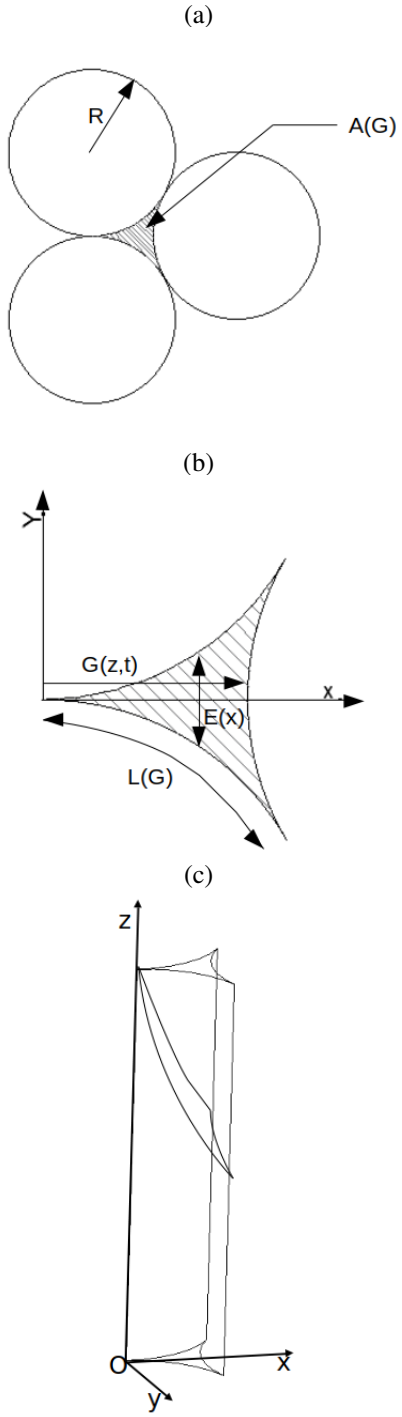

Figure 2: (a) Schematic view of the interstice formed by three circular capillaries (b) Horizontal cross sectional view of meniscus in the interstice (c) 3-D view of meniscus inside the interstice

Let $A'(G) = \partial A/\partial G$ which from (6),is,

$$A'(G) = 2(R - \sqrt{R^2 - G^2}). \tag{6}$$

Hereinafter $'$ indicates derivative w.r.t. G. Now using mass conservation equation,

$$\partial A(G)/\partial t = A'\dot{G} = -\partial Q/\partial z \tag{7}$$

where $Q(z,t)$ is the volume flux of fluid flowing in the z-direction.

To evaluate $\dot{F}$ in (3), we find the free energy of the system as the sum of gravitational energy and interfacial energy.

$$F(G) = \int_0^{z_m} \{\rho g A(G) \cdot z - 2L(G)\sigma\cos\theta\} dz \tag{8}$$

where σ is the surface tension, θ is the contact angle and $L(G)$ is the length of the curve for $0 < x < G$ shown in the Figure 2(b)

$$L(G) = \int_0^G \sqrt{1 + \frac{1}{4}\left(\frac{dE(x)}{dx}\right)^2} dx \tag{9}$$

After substituting (2) in (9),

$$L(G) = R\sin^{-1}(G/R) \tag{10}$$

and therefore

$$L'(G) = \left(1 - \frac{G^2}{R^2}\right)^{-1/2}. \tag{11}$$

From (8),

$$\dot{F}(G) = \int_0^{z_m} \left(\rho g A' z - 2L'\sigma\cos\theta\right)\dot{G} dz. \tag{12}$$

Integrating (12) by parts and using equation (7), we get,

$$\dot{F} = \int_0^{Z_m} \left(\rho g - 2\frac{\partial\left(L'/A'\right)}{\partial z}\sigma\cos\theta\right) Q dz. \tag{13}$$

We now obtain the expression for the dissipation function ϕ in (3) using lubrication approximation. The velocity in z-direction v_z is determined by Stoke's equation.

$$\mu\left(\frac{\partial^2}{\partial x^2} + \frac{\partial^2}{\partial y^2}\right) v_z = -\frac{\partial P}{\partial z} - \rho g, \tag{14}$$

with the boundary conditions are $v_z = 0$ at boundary $y = \pm E(x)/2$. Solving (14) analytically, we get a parabolic profile for the flow as,

$$v_z(x,y,z,t) = \frac{3}{2}\bar{v}_z(x,z,t)\left[1 - \left(\frac{2y}{E(x)}\right)^2\right], \tag{15}$$

where $\bar{v}_z(x,z,t)$ is the y-averaged velocity. The flux is calculated by integrating the velocity over the area as,

$$Q(z) = \int_0^{G(z)} E(x)\bar{v}_z(x,z,t) dx. \tag{16}$$

In channel flow,

$$\bar{v}_z(x,z,t) = C(z,t)E^2(x) \tag{17}$$

where $C(z,t)$ is proportionality constant, then

$$Q(z) = \int_0^{G(z)} E^3(x)C(z,t) dx. \tag{18}$$

In other words,

$$Q(z) = B(G)C(z,t), \tag{19}$$

where

$$B(G) = \int_0^G E^3(x) dx. \tag{20}$$

Evaluating $B(G)$ using (2) and (20)

$$B(G) = -15R^4\arcsin(G/R) + 32R^3G - 17R^2G\sqrt{R^2 - G^2} + 2G^3\sqrt{R^2 - G^2} - 8RG^3. \tag{21}$$

Expanding (21) as a Taylor series for small G/R, we get,

$$B(G) \simeq \frac{1}{7}\frac{G^7}{R^3} \tag{22}$$

The dissipation function Φ is

$$\Phi = \frac{1}{2}\int_0^{Z_m}\int_0^{G(z)} \frac{12\mu}{E(x)}\bar{v}_z(x,z,t) dz dx, \tag{23}$$

which using (17) and (19), simplify to

$$\Phi = \frac{1}{2}\int_0^{Z_m} \frac{12\mu}{B} Q^2(z) dz \tag{24}$$

Substituting (13) and (23) in (3), the Rayleighian becomes

$$R = \int_0^{Z_m} \left(\rho g - 2\frac{\partial\left(L'/A'\right)}{\partial z}\sigma\cos\theta\right) Q dz + \frac{1}{2}\int_0^{Z_m} \frac{12\mu}{B} Q^2(z) dz \tag{25}$$

Using Onsager's principle, $\delta R/\delta Q = 0$

$$Q = \frac{B}{12\mu}\left(-\rho g + 2\sigma\cos\theta\frac{\partial\left(L'/A'\right)}{\partial z}\right). \tag{26}$$

Using (7) and (26),

$$\dot{G} = \frac{1}{A'}\frac{\partial}{\partial z}\left(\frac{B}{12\mu}\left(\rho g - 2\sigma\cos\theta\frac{\partial\left(L'/A'\right)}{\partial z}\right)\right). \tag{27}$$

Inserting the values of A', B and L' in (27) from (6),(22) and (11) and taking the binomial approximation, we get the final time evolution equation for the dimensionless meniscus thickness as,

$$\frac{\partial(G/R)}{\partial t} = \frac{-\rho g R^2}{84\mu}\frac{1}{(G/R)^2} \frac{\partial}{\partial z}\left[\left(\frac{G}{R}\right)^7\left(1 - \left(\frac{2\sigma\cos\theta}{R\rho g}\right)\frac{\partial}{\partial z}\left(\frac{G}{R}\right)^2\right)\right] \tag{28}$$

We choose R as the characteristic length scale in x direction and

$$H_c = \frac{2\sigma\cos\theta}{R\rho g} \tag{29}$$

as the characteristic length scale in the z-direction. The characteristic time is chosen as

$$t_c = \frac{84\mu H_c}{\rho g R^2}. \tag{30}$$

Rewriting (28) in dimensionless form

$$\frac{\partial \tilde{G}}{\partial \tilde{t}} = -7\tilde{G}^4 \frac{\partial \tilde{G}}{\partial \tilde{z}} - 8\tilde{G}\left(\frac{\partial \tilde{G}}{\partial \tilde{z}}\right)^2 - 2\tilde{G}^2\left(\frac{\partial^2 \tilde{G}}{\partial^2 \tilde{z}}\right) \tag{31}$$

where

$$\tilde{G} = \frac{G}{R}$$
$$\tilde{z} = \frac{z}{H_c}$$
$$\tilde{t} = \frac{t}{t_c}$$

For self-similar solution of (31), we assume

$$\tilde{G}(\tilde{z}, \tilde{t}) = F(\chi)\tilde{t}^{\alpha} \tag{32}$$

where

$$\chi = \tilde{z}\tilde{t}^{\beta} \tag{33}$$

Here, α and β are some parameters. Substituting (32) and (33)in (31), we obtain,

$$(F'\chi\beta + F\alpha)\tilde{t}^{(\alpha-1)} = -7F^4F'\tilde{t}^{(5\alpha+\beta)} - (8FF'^2 + FF'')\tilde{t}^{(3\alpha+2\beta)} \tag{34}$$

The above equation becomes time independent when,

$$\alpha - 1 = 5\alpha + \beta = 3\alpha + 2\beta \tag{35}$$

i.e. when

$$\alpha = \frac{-1}{6} \quad \& \quad \beta = \frac{-1}{3}. \tag{36}$$

At the tip of the corner meniscus, $\tilde{z} = \tilde{Z}_m$ and $\chi = \chi_o$. Using (36) in (33), we then obtain

$$\tilde{Z}_m = \chi_o \tilde{t}^{(1/3)} \tag{37}$$

as the scaling for the tip of the corner meniscus. The scaling law implied by (37) is

$$\frac{Z_m}{H_c} = \chi_o \left(\frac{t}{t_c}\right)^{1/3}, \tag{38}$$

where H_c and t_c are given by (29) and (30) respectively. Substituting (29) and (30) in (38) implies that

$$Z_m = C\left(\frac{t\,(\sigma\cos\theta)^2}{\rho\mu g}\right)^{1/3}, \tag{39}$$

where $C = \chi_o(2/(168)^{1/3})$

Table 1: **The values of the parameters**

$\sigma(N/m)$	$\mu(Pa-s)$	$\rho(Kg/m^3)$	θ(deg)
0.071	$8.4*10^{-4}$	997	45

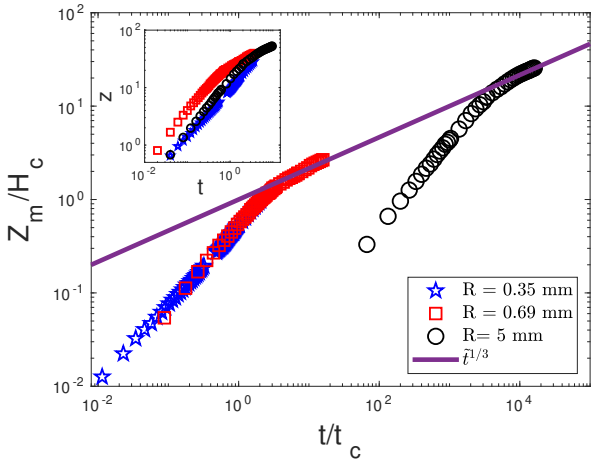

Figure 3: **Variation of the dimensionless corner height with the dimensionless time for three different capillaries**

IV. RESULTS AND DISCUSSION

The Figure 3 shows plot between the dimensionless corner height rise $\tilde{Z}_m$ verses dimensionless time $\tilde{t}$. At the later time periods, where gravity and viscous effects becomes dominant balanced by surface tension force, the measured $\tilde{Z}_m$ for R= 690 μm and R = 5000 μm collapse on to (39). At the initial time stages, the experimental plot shows a steeper slope, the rate of capillary rise at the corner is then faster in this initial regime compared to the later regime. The gravitational effects become negligible here. The experimental results for the smallest two capillaries overlap each other in this initial time period. However, for the larger capillary, there is a shift in this initial regime. Scaling results for this initial regime is yet unknown.

V. CONCLUSIONS

In the present work, we developed a scaling law for the capillary rise of the liquid in the corner of an interstice created by an array of circular capillary tubes/rods. Using the minimisation of sum of free energy and viscous dissipation using Onsager's principle, the capillary height was shown to scale as $Z_m = \left(\frac{t(\sigma\cos\theta)^2}{\rho\mu g}\right)^{1/3}$, independent of the radius of the capillary tube/rod. The measurements of capillary heights in the interstitial corners of capillary bundles of 3 sizes showed an initial regime with a higher rate of rise, and a later regime with a lower rate of rise. the proposed scaling law matched the behaviour of the corner rise in the later regime.

ACKNOWLEDGEMENTS

We gratefully acknowledge the financial support of DST, Government of India through their grant IMP/2018/001167.

We acknowledge the support of Usha P Verma Sc 'G', Advanced Systems Laboratory (ASL), DRDO, and Astra Microwave Products Ltd.

NOMENCLATURE

g	Gravity	$[ms^{-2}]$
σ	Surface temsion	$[Nm^{-1}]$
μ	Dynamic viscosity	$[Pa-s]$
ρ	Density of liquid	$[Kgm^{-3}]$
R	Radius of the capillary	$[m]$
θ	Static contact angle	$[degree]$
h	Height of the meniscus	$[m]$
t	Time	$[sec]$
t_c	Time scale	$[sec]$
$L(G)$	Length of one curve y	$[m]$
$A(G)$	Cross-sectional area of interstice	$[m^2]$
H_c	Length scale along z direction	$[m]$
D	Diameter of the capillary	$[m]$
C	Constant	[-]
P	Pressure	$[Nm^{-2}]$
Q	Volume flux along z direction	$[m^3s^{-1}]$

REFERENCES

[1] M. Dong and I. Chatzis, *The imbibition and flow of a wetting liquid along the corners of a square capillary tube*, J.of Colloid and Interface Science **172** (1995), 278–288.

[2] F.J.Higuera, A.Medina, and A. Linan, *Capillary rise of a liquid between two vertical plates making small angle*, Physics of Fluids **20** (2008), 102–109.

[3] Alexandre Ponomarenko, David Quere, and Christophe Clanet, *A universal law for capillary rise in corners*, J. Fluid Mech. **666** (2011), 146–154.

[4] Jiajia Zhou and Masao Doi, *Universality of capillary rising in corners*, J. Fluid Mech. **900** (2020), A29–43.